water

MDPI

Article

Assessing the Coordinated Operation of Reservoirs and Weirs for Sustainable Water Management in the Geum River Basin under Climate Change

Jung Min Ahn, Deuk Seok Yang, Kang Young Jung and Dong Seok Shin *

National Institute of Environmental Research Nakdong River Environment Research Center, 24, Pyeongri-1gil, Dasan-myeon, Goryeong-gun, Gyeongsangbuk-do 40103, Korea; ahnjm80@gmail.com (J.M.A.); yds7055@korea.kr (D.S.Y.); happy3313@korea.kr (K.Y.J.)

* Correspondence: sds8488@korea.kr; Tel.: +82-54-950-9700

Received: 16 November 2017; Accepted: 22 December 2017; Published: 2 January 2018

Abstract: In this study, an integrated system for the comprehensive analysis of climate change, runoff, reservoir operation, and power generation was developed. In order to apply reliable climate change scenarios to the Geum River Basin, we applied representative concentration pathway (RCP) scenarios adopted by the Intergovernmental Panel on Climate Change for its fifth assessment report in 2014 to the streamflow synthesis and reservoir regulation model at a regional scale with 1-km spatial resolution to analyze future runoff. This analyzed future runoff was applied to the Hydrologic Engineering Center—Reservoir System Simulation to analyze the hydrological behavior caused by reservoir operation through flow duration analysis at each of several important points. The objective was to provide initial data suitable for future basin management through an examination of power generation. Applying the RCP 4.5 and 8.5 scenarios showed that runoff would increase continuously compared with the past. However, in the RCP 8.5 scenario (where carbon reductions have not been achieved), runoff from flooding would be reduced considerably. It was found that power generation would be reduced compared with the past under the climate change scenarios, but additional power generation could be realized with the coordinated operation of reservoirs and weirs. These results suggest that, despite climate change, the risk to power generation could be reduced with the coordinated operation of reservoirs and weirs.

Keywords: climate change; generation; SSARR; HEC-ResSim; Geum River

1. Introduction

The fourth and fifth assessment reports by the Intergovernmental Panel on Climate Change (IPCC) state that observational data show that global warming is indisputable and the future climate will cause frequent severe droughts and flooding events that will challenge water resource management [1]. By convention, climate change is defined as "represent(ing) a statistically significant climate change that lasts for decades or more", and the future hydrological environment will respond to reflect any such change. For example, from 1998 to 2007, rainfall in Korea during the rainy season increased considerably compared with previous years [2].

A great deal of research has been undertaken in Korea to minimize the effects of climate change. Policies on climate change have been established and enacted, starting with the 1st Convention on Integrated Government Strategy for Climate Change in 1999 and including the National Climate Change Response Strategy of 2011–2015, which was established through the Basic Law for Low Carbon Green Growth [3]. Following basic research and a comprehensive assessment of the effects of climate change on basin environments, the National Institute of Environmental Research [4,5] established a plan to address climate change in Korea that was published as a white paper. The Korea Rural

Economic Institute [6] performed research on agricultural responses to climate change and published its findings in the Nonghyup Economic Research Institute report. To manage dispersed climate data and to construct infrastructure for national use, the Korea Meteorological Association established the Climate Change Information Center in 2011. It manages various climate data, produced both domestically and internationally, and it makes them available for anyone to use. This supports various projects on climate change research, particularly in the field of water resources. This is important because it is expected that not only will localized heavy rainfall occur in response to climate change, brought about by increases in atmospheric greenhouse gases, but vulnerability to floods and droughts will also increase.

Integrated water resource management is considered necessary as a climate change adaptation measure; thus, a large-scale integrated regional water management program was established by region and is now in operation [7]. When integrated water management is centered on flood control, it is called integrated flood management. This has been studied with great interest, and there have been many attempts to implement it throughout the world [8]. To adapt to the prospect of severe climate change in the future, Korea will require a robust water management strategy. However, to be able to respond to future water resource problems, it is necessary to first understand and evaluate the quantifiable effects that climate change is having on current water resources.

To evaluate fully the effects of climate change, many elements must be considered sequentially, including climate change scenarios, general circulation models (GCMs), downscaling techniques, rainfall/runoff models, reservoir operation models, and environment evaluation models; as each element is considered, uncertainty gradually increases. Since this uncertainty will impact the adaptation strategies adopted to mitigate the effects of future climate change, research that can recognize and reduce the associated uncertainty is needed [9]. Research has been performed in Korea on the hydrological evaluation of basins with regard to future climate change [10,11]. However, because this research has used different elements (i.e., emissions scenarios, GCMs, hydrological models, and downscaling techniques) and because of inherent uncertainties, markedly different results have been obtained for the same basin. Thus, the derived results cannot be applied to real, relevant policies [12].

By tracking reservoirs in the Peribonka River Basin (Canada), Minville et al. [13] examined irrigation, flooding, and water generation capacity under an uncertain future climate using the Hydrologic Engineering Center—Reservoir System Simulation (HEC-ResSim) reservoir modeling software [14]. Fang et al. [15] studied the optimization of dam operations during drought by classifying climate conditions and irrigation and flooding seasons, thereby controlling the water supply volume and minimizing the water deficit in the Huanghe–Huaige water system (China). Divakar et al. [16] studied the total benefit functions for agriculture, hydropower, and the domestic and industrial sectors under a case study for allocation practices in Thailand. Lin and Rutten [17] studied the optimal operation of a network of multipurpose reservoirs for real-time control based on the application of modeled predictive control of a reservoir system. Li et al. [18] studied an improved multi-objective optimization model for supporting the reservoir operations of China's South–North Water Transfer Project.

To examine the integrated operation of an existing dam and 16 multifunctional weirs constructed under the Four Rivers Restoration Project, Ahn et al. [19] studied the connected operation of an existing dam and three multifunctional weirs by applying the HEC-ResSim model to the Geum River Basin, suggesting an operational rule for the multifunctional weirs in order to analyze the environmental flow and hydropower. In this research, we evaluated the amounts of basin runoff and power generation resulting from climate change and the operation of hydraulic structures. To ensure we implemented a reliable climate change scenario in the Geum River Basin (Korea), we used regional-scale RCP scenarios with 1-km spatial resolution, provided by the Climate Change Information Center [20], and we applied them to a streamflow synthesis and reservoir regulation (SSARR) model to analyze future runoff. An integrated simulation of the runoff results was performed using HEC-ResSim, and we evaluated the potential for future power generation resulting from the coordinated operation of reservoirs and multifunctional weirs.

2. Materials and Methods

2.1. Target Basin

The area of the Geum River Basin, which is the focus of this research, is 9915 km^2, with a main stream length of 395.9 km. The main tributaries within the basin (from upstream to downstream) are the Namdae, Bonghwang, Song, Kap, Miho, Yugu, Ji and Nonsan streams. Except for the Miho stream, these are all small streams with basins no greater than 3–6% of the main basin area.

In order to obtain highly reliable hydrological data, this research focused on the Geum River Basin water system, which is one of the four largest river basins in Korea, where basin examinations and on-site examinations have been performed over several years. As it is difficult to understand the regional runoff situation when analyzing an entire river basin, we divided it into smaller basins, based on major watermark points at multipurpose dams, principal streams, and tributaries. The ARC-GIS (geographic information system) tool was used to reflect the characteristics of the small basins that were affected by each hydraulic facility, and a 1:25,000 digital map based on the main control points of the Geum River Basin was used to create a 30 × 30 m digital elevation model. As shown in Figure 1, the Geum River Basin was divided into 14 parts, and maps of the equivalent scale of soil type and land usage were used to define the characteristics of the basins and channels of each part.

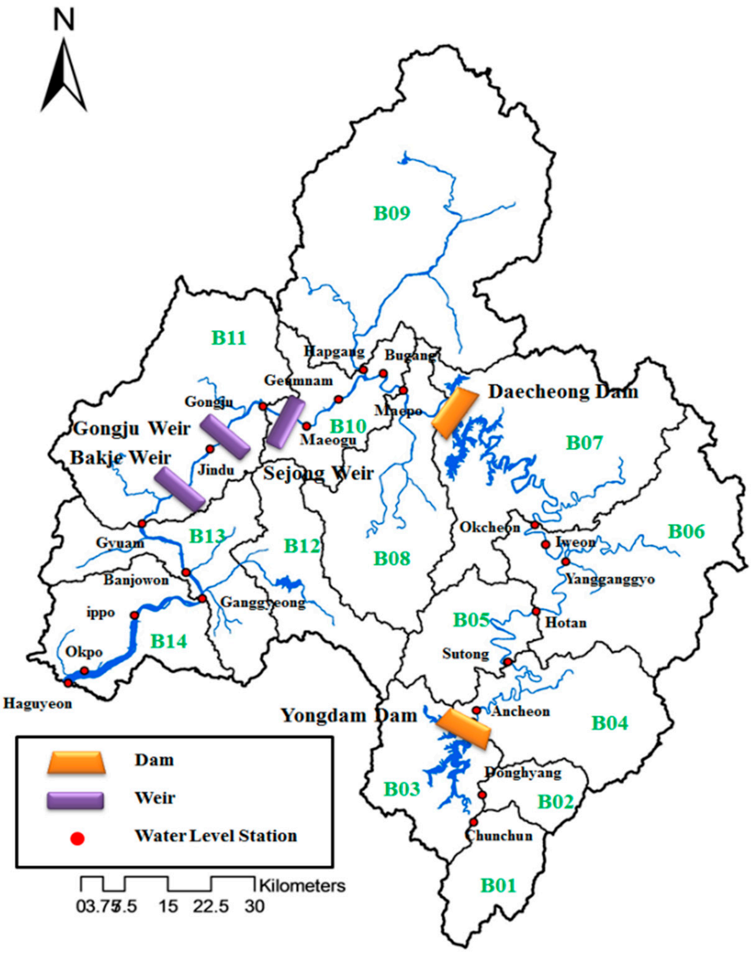

Figure 1. Study area.

As shown in Figure 2, to evaluate the river environment according to changes in the hydrological basin environment, we used observed data and climate change data for our atmospheric data, the SSARR model for our basin hydrological analysis model, and HEC-ResSim for our hydraulic facility operation model.

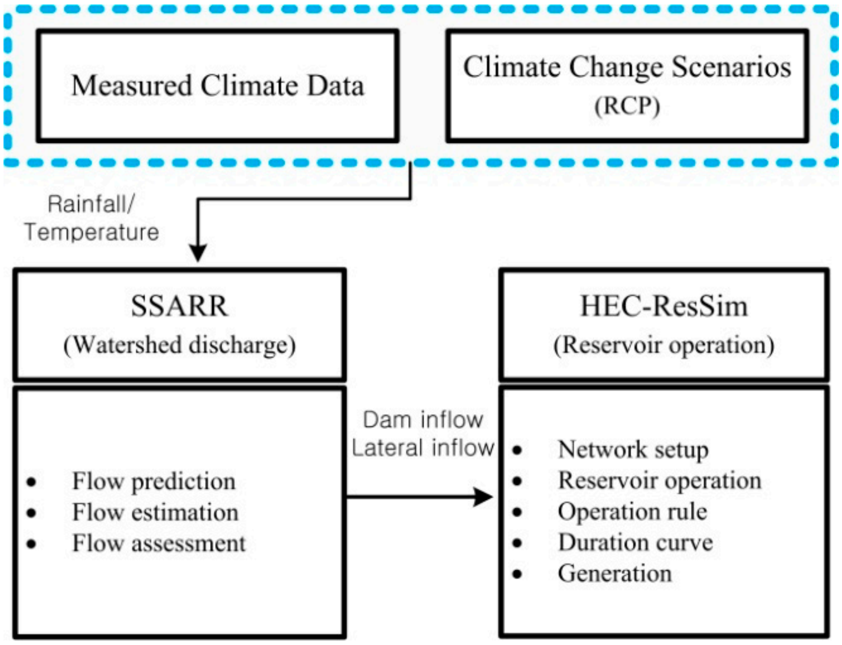

Figure 2. Model linking process.

2.2. Climate Change Scenarios

Climate change is occurring now, and it is believed that it will continue and even accelerate in the future [1]. Therefore, new climate scenarios are needed for use in a variety of fields that can incorporate fresh data, improve accuracy, and overcome the resolution problems of the greenhouse gas emissions scenarios used in the fourth assessment report of the IPCC. Thus, in September 2007, representative concentration pathway (RCP) scenarios were developed by experts on the IPCC as global standard greenhouse gas concentration scenarios. Four representative concentrations were selected, and the corresponding scenarios were produced. These four selected concentrations were named, based on their radiative forcing (W/m^2), as RCP 2.6, 4.5, 6.0 and 8.5 [21].

In the emission scenarios used in the fourth assessment report of the IPCC, the form future societies and economies would take dictated suitable emissions scenarios and greenhouse gas concentrations. In this type of sequential process, time delays occur as information is transmitted between each separate scenario [1]. For the RCPs, the greenhouse gas concentrations were chosen based on the amount of forcing in the atmosphere due to human activity via the new greenhouse gas emissions scenarios adopted in the fifth assessment report of the IPCC [22]. For a single representative radiative forcing scenario, there can be several socioeconomic scenarios, and the word "representative" means it is one of several different scenarios that have similar radiative forcing and emission characteristics. Furthermore, greenhouse gas concentrations change over time; thus, the word "pathway" was introduced to emphasize its dynamic nature [22].

The RCP scenario numbers refer to the level of radiative forcing, which is the degree to which greenhouse gasses affect the energy balance. The amount of solar radiation that reaches the surface of the earth is approximately 238 W/m^2; therefore, the radiative forcing of RCPs 8.5, 6.0, 4.5 and 2.6 correspond to incident solar radiation amounts of approximately 3.6%, 2.5%, 1.9% and 1.1%, respectively. The South Korean climate change scenario with 1-km resolution was created through a process of statistical downscaling, based on the climate change scenarios for the Korean Peninsula

(12.5 km) created through regional climate models. The distinct features of the RCP scenarios are as follows. Under RCP 2.6, it is possible for the earth to recover on its own from the effects of human activities. Under RCP 4.5, policies for greenhouse gas reduction are considered reasonably effective. Under RCP 6.0, policies for greenhouse gas reduction are considered somewhat effective. Under RCP 8.5, emissions of greenhouse gasses are considered similar to current trends.

The Climate Change Information Center provides climate change data for 73 major points and 230 cities/localities in Korea. The data for the major points are the values of the closest grid points, whereas the data for the 230 cities/localities are the mean values for the area. Furthermore, only information for RCPs 4.5 and 8.5, with a control integral of 200 years, is provided. RCP climate change information considers 2005 to be the initial conditions, and it simulates change from 2006 onward. In this research, we chose RCPs 4.5 and 8.5 to evaluate the possible future hydrological environment that could occur if greenhouse gas emissions were reduced or maintained at current levels.

As shown in Figure 3, 14 observatories were chosen from the observatories operated by the Korea Meteorological Association in the Geum River Basin. The observatories are as follows: Jangsu = A, Geumsan = B, Geochang = C, Jeonju = D, Chupungryeong = E, Boeun = F, Daejeon = G, Cheongju = H, Cheonan = I, Icheon = J, Chungju = K, Boryeong = L, Buyeo = M and Gunsan = N. As shown in Table 1, the Thiessen method, which is known to be more accurate than normal arithmetic mean methods, was used to choose control areas for each observatory and to find appropriate weights for those areas. The mean spatiotemporal rainfall for the 14 observatories in 10-year increments is shown in Figure 4. Under RCP 4.5, rainfall increases slowly until 2080 when the rainfall exceeds 1500 mm; however, under RCP 8.5, the rainfall exceeds 1500 mm in 2040. Thus, it is evident that climate change happens more quickly under RCP 8.5.

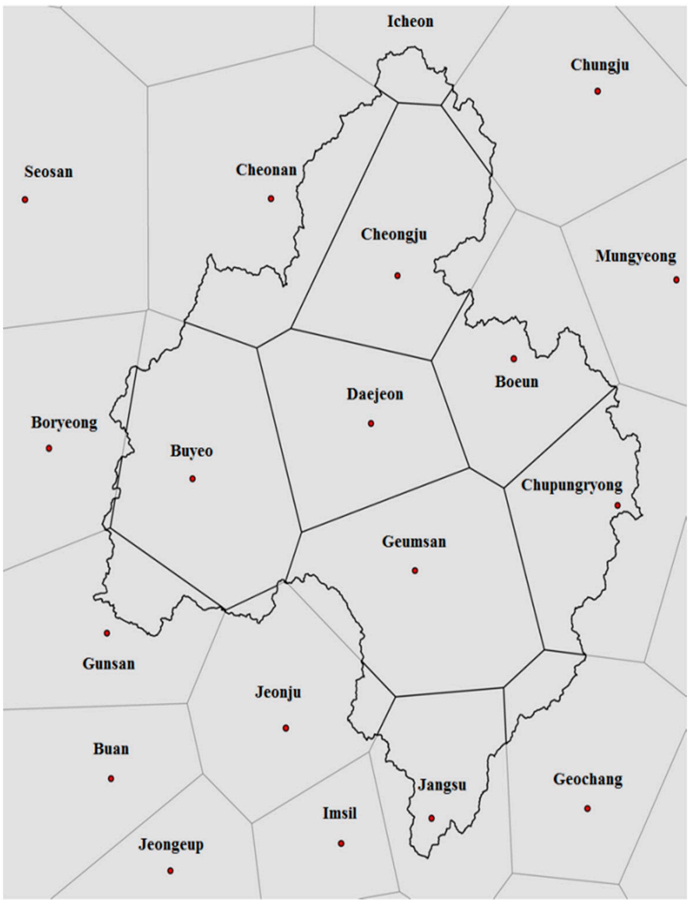

Figure 3. Thiessen polygons in the Geum River Basin using ARC-GIS.

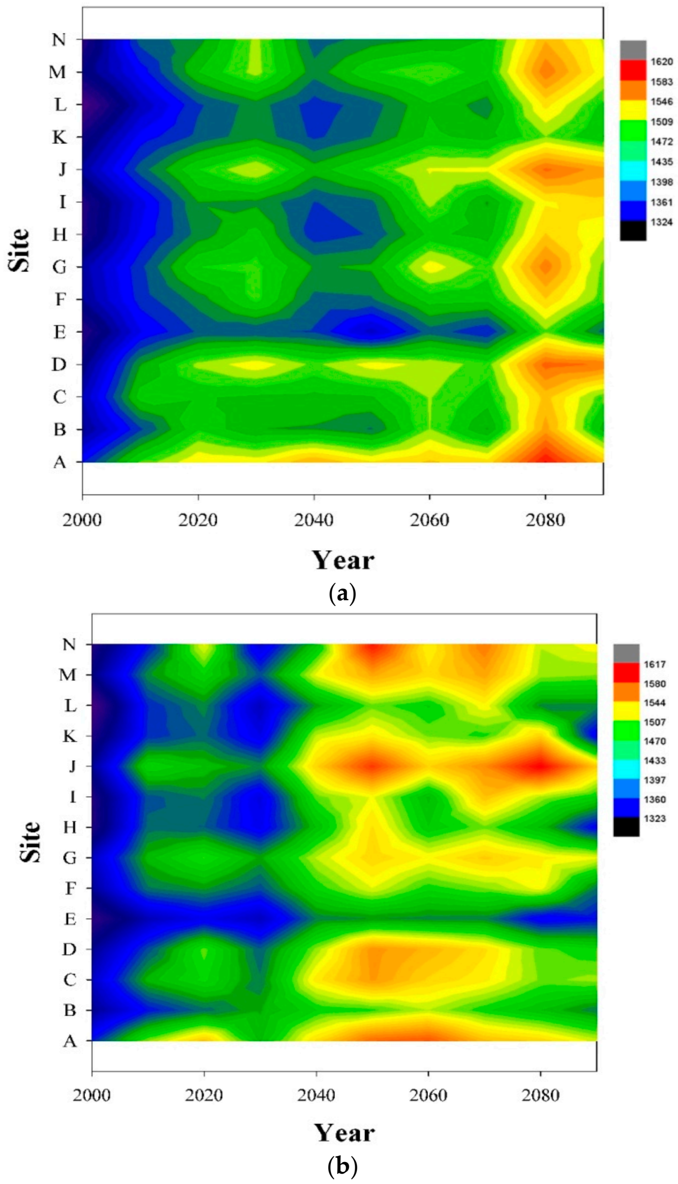

Figure 4. Spatiotemporal change of rainfall under RCP scenarios: (**a**) RCP 4.5; (**b**) RCP 8.5.

Table 1. Thiessen coefficients.

Sub Basin	Station	Area (km^2)	Thiessen Coefficient	Sub Basin	Station	Area (km^2)	Thiessen Coefficient
B01	Jangsu	291.1	1.00	B09	Cheonan	399.7	0.22
B02	Jangsu	138.8	0.84		Boeun	17.5	0.01
	Geochang	26.5	0.16		Cheongju	1224.5	0.66
B03	Geumsan	202.6	0.43		Icheon	135.7	0.07
	Jangsu	179.8	0.38		Chungju	71.3	0.04
	Jeonju	90.5	0.19	B10	Daejeon	331.5	0.79
B04	Geumsan	390.4	0.62		Chungju	72.4	0.17
	Geochang	132.6	0.21		Cheonan	16.9	0.04
	Chupungryong	97.3	0.17	B11	Cheonan	276.4	0.25
B05	Geumsan	374.8	1.00		Buyeo	741.0	0.67

Table 1. *Cont.*

Sub Basin	Station	Area (km^2)	Thiessen Coefficient	Sub Basin	Station	Area (km^2)	Thiessen Coefficient
B06	Geumsan	244.9	0.23	B11	Boryeong	30.2	0.02
	Chupungryong	775.1	0.73		Daejeon	66.2	0.06
	Boeun	37.8	0.04	B12	Geumsan	198.8	0.43
B07	Geumsan	108.6	0.09		Buyeo	145.2	0.31
	Chupungryong	25.2	0.02		Daejeon	123.1	0.26
	Boeun	800.7	0.67	B13	Jeonju	29.6	0.05
	Daejeon	228.2	0.19		Boryeong	10.7	0.02
	Cheongju	36.7	0.03		Buyeo	541.2	0.93
B08	Geumsan	195.4	0.26	B14	Buyeo	271.8	0.51
	Daejeon	523.2	0.70		Jeonju	9.1	0.02
	Cheongju	36.7	0.04		Gunsan	250.7	0.47

2.3. Basin Runoff Model

2.3.1. Model Construction

The hydrometeorological parameters were initialized by basin, and they included rainfall data, rainfall adjustment by elevation, evapotranspiration index (ETI), ETI adjustment by rainfall intensity (EKE), ETI adjustment by temperature, ETI adjustment by soil moisture index (SMI), ETI adjustment by SMI (DKE), ETI adjustment by elevation (ETEL), ETI adjustment by month (ETM), maximum interception (TINTMX), and temperature data. Initial values were set for the following internal processing parameters: runoff percent by SMI (SMI-ROP), baseflow percent by baseflow infiltration index (BII-BFP), surface water and subsurface water (S-SS), BII time of storage (BIITS), time delay or time of storage for the calculation of change in BII (typical values range from 30 h to 60 h), maximum value for BII (BIIMX), baseflow input limit value (BFLIM; if total base flow input rate (TBF) is greater than BFLIM, set TBF to BFLIM), percent of baseflow limit to cover the lower zone (PBLZ; percentage of the total base flow going to lower zone routing, with a typical value of 50%), and the maximum value of this (DGWLIM).

The SMI is used to determine runoff as an indicator of the relative soil wetness. The generated runoff for a period (RGP) is computed as the product of moisture input (MI) and ROP. The ROP from the SMI table and the MI from the snow pack or precipitation are used to calculate the total generated runoff for a period (RGP). When the soil moisture is depleted to approximately the permanent wilting point, the SMI is a small number that yields little to no runoff. When precipitation recharges the soil moisture, the value of the SMI increases until it reaches a maximum value considered to represent its field capacity or water holding capacity. At this value, the ROP would approach 100%. The SMI is depleted only by the ETI. The BII-BFP shows the relationship between the BII and BFP to calculate the base flow component. BII may be thought of as an index of depression storage, which holds runoff available for deep percolation. S-SS represents the relationship between the surface runoff input rate (RS) and the total input rate (RGS) to surface and sub-surface runoff. SSS is a type of RGS. The time of storage for the surface runoff component (TS) is used to route surface flow with a specified number of increments of storage that can be considered a series of small lakes that delay runoff. The time of storage for the sub-surface runoff component (TSS) is used to route sub-surface flow with a specified number of increments of storage that can be considered a series of small lakes that delay runoff.

The basin tracing of the SSARR model is achieved with independent traces on four flow fields: surface water, infiltration water, subsurface water, and additional returning subsurface water in the integrated snow band basin model. It is assumed that each flow field is composed of several virtual linear reservoirs, and reservoir traces were performed for each of these. The parameters for each flow field included the number and storage time of each virtual reservoir, and the initial values for each parameter were selected by referring to the basin area, principal stream length, and arrival time.

As in the basin trace, a trace method of continuous virtual reservoirs was used for the stream trace. The parameters included the number and storage time of each virtual reservoir, which were set using formulas developed by the United States Bureau of Reclamation. In the stream trace concept used by the SSARR model, the storage time is entered directly, but, in the stream model, the storage time is expressed by the flow function shown in Equation (1). The basin model in the SSARR model is linear, but the stream model, including the reservoirs, is nonlinear.

$$\mathrm{T_s} = \frac{\mathrm{KTS}}{\mathrm{I^n}} \quad (1)$$

Here, the parameters are the number of virtual reservoirs, and the storage time for each reservoir ($\mathrm{T_s}$). KTS is a constant determined by trial and error, I is the inflow rate, and n is a coefficient with a value between −1 and 1.

The water taken in from the basin or streams can be divided into that which returns to the basin or stream and that which drains to another basin or another stream. This rate of return (return rate and drainage rate) is a very important factor for analyzing the hydrological balance of streams. However, the return amount was calculated from the water intake ratio (return rate), as there are no simultaneously observed values for the intake amount and the flow for calculating the return amount in the Geum River Basin. The return rate due to inflow differs according to water usage, and it changes greatly by season. Therefore, the values of the return rate and the drainage rate for fresh/public water used in the Geum River Basin were assumed to be 80% and 60%, respectively. For the return rate of agricultural water, it was assumed to be 30–40% in the peak season (March–August) and 60–80% in the off season (September–November). A schematic of the SSARR model is shown in Figure 5.

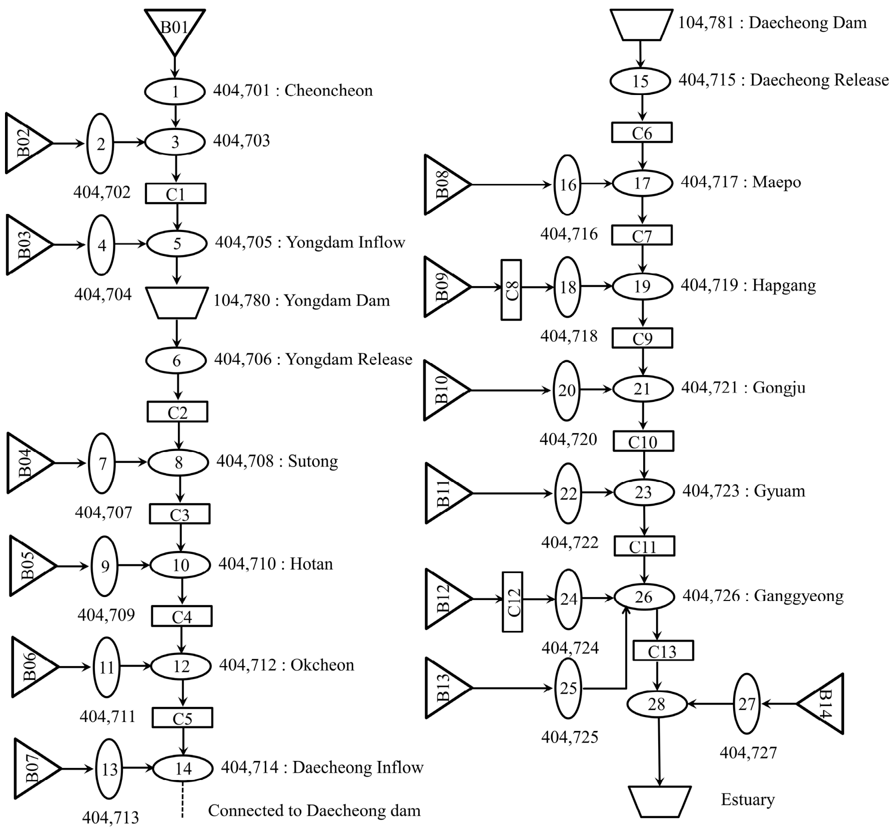

Figure 5. Schematic of the SSARR model.

2.3.2. Model Revision and Verification

In this study, we calculated the SMI-ROP and BII-BFP based on flow observations made in the Geum River Basin from 2001 to 2008 (Figures 6 and 7). The ultimate parameters were revised into annual units and subsequently determined by dividing them into high-water levels and low-water levels, then combining these. The runoff rate according to soil moisture has limitations in adjusting the peak flow and the overall runoff, but it is an important parameter. The subsurface inflow rate by infiltration is a parameter that determines the ratio of the subsurface inflow to the total runoff. The SMI and BII, which are related to the basin tracing, were both found to be sensitive to high-water and low-water levels. A comparison of cases in which the surface and subsurface water storage times were a function of the flow amount and those in which they were fixed as constants revealed results that were sensitive not only during times of low water but also during times of high water. We believe these two parameters can be manipulated to adjust the peak flow and total runoff, to increase the reliability of the runoff results.

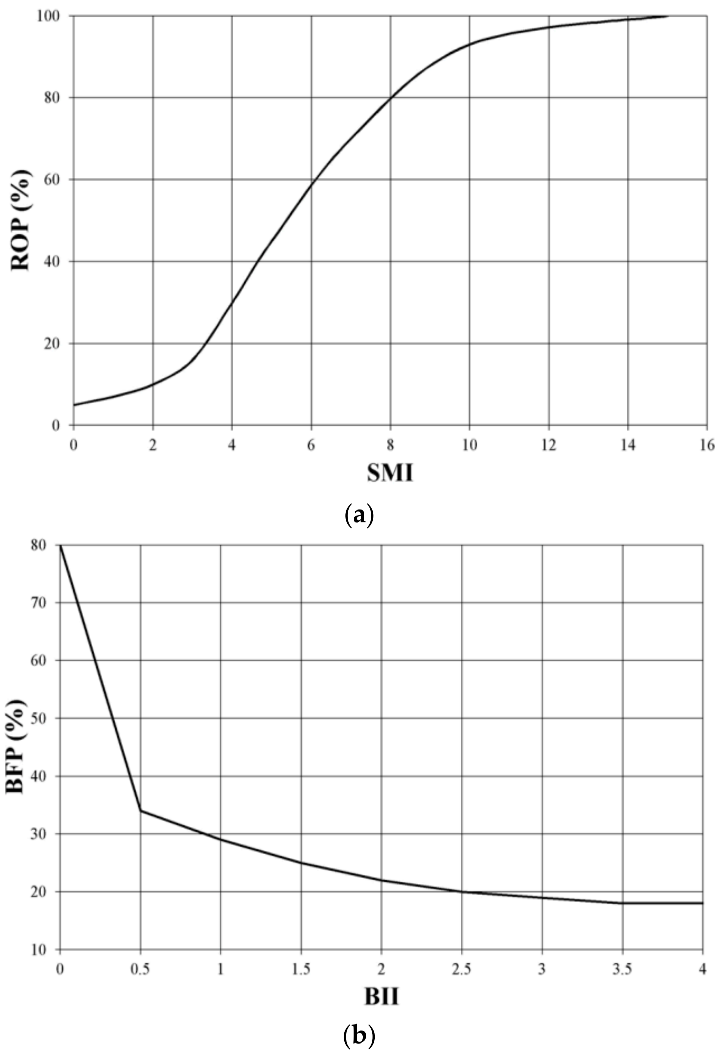

Figure 6. Parameters of SMI-ROP and BII-BFP applied to the SSARR model: (**a**) SMI-ROP; (**b**) BII-BFP [23].

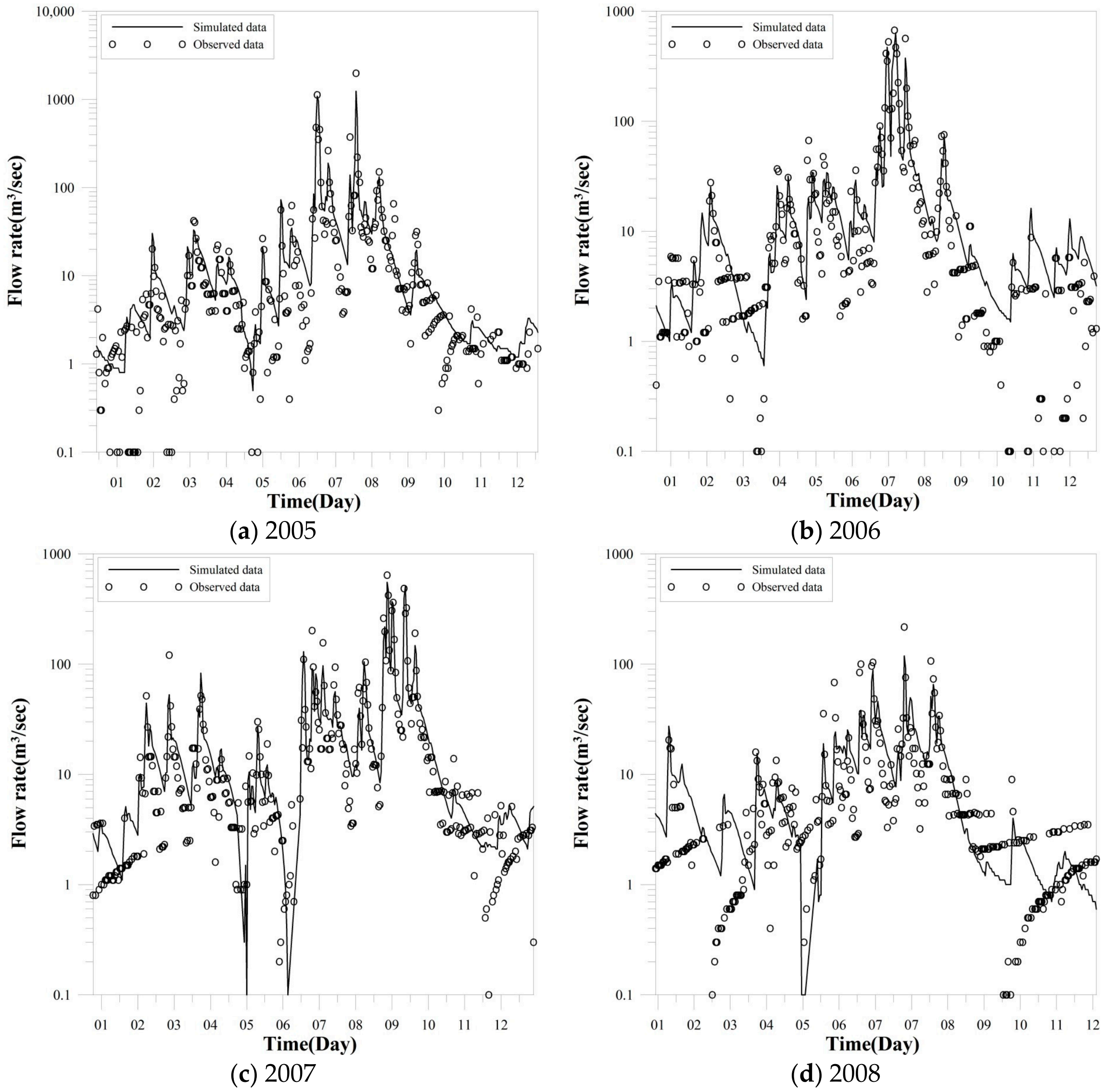

Figure 7. Calibration results of the SSARR model for each year

The parameters of the model consist of values established through research by Ahn et al. [23]. The root mean square error (*RMSE*) depends on the scale of the dependent variable. It should be used as a relative measure to compare forecasts for the same series across different results. The smaller the error, the better the forecasting ability of that model, according to the *RMSE* criterion. These individual differences are also called residuals, and the *RMSE* serves to aggregate them into a single measure of predictive power. The Nash–Sutcliffe model efficiency coefficient (*NSEC*) [24] is used to assess the predictive power of hydrological models. The *NSEC* can range from $-\infty$ to 1. An efficiency of 1 (*NSEC* = 1) corresponds to a perfect match of modeled discharge to the observed data. An efficiency of 0 indicates that the model predictions are as accurate as the mean of the observed data, whereas an efficiency less than zero ($-\infty < NSEC < 0$) occurs when the observed mean is a better predictor than is the model. The United States Geological Survey reported that the Cedar River Basin model meets the criterion of having an *NSEC* greater than 0.5, and is a good fit for the streamflow conditions for the calibration period [25]. The Theil inequality coefficient is such that it will always lie between 0 and 1. If TIC = 0, $X_{model,i} = X_{obs,i}$ for all forecasts, and there is a perfect fit; if TIC = 1 the predictive performance is as bad as possible. The corresponding equations are shown below.

$$RMSE = \sqrt{\frac{\sum_{i=1}^{n}(X_{model,i} - X_{obs,i})^2}{n}} \quad (2)$$

$$NSEC = 1 - \frac{\sum_{i=1}^{n}(X_{model,i} - X_{obs,i})^2}{\sum_{i=1}^{n}(X_{obs,i} - \overline{X}_{obs})^2} \quad (3)$$

where $X_{obs,i}$ represents the observed values, $X_{model,i}$ are the modeled values at time/place i, and $\overline{X}_{obs}$ are the average observed values.

Satisfactory model efficiency can then be established depending on the number of times (N_t) that the observation's variability is greater than the mean error. If the mean model error is represented by the $RMSE$, and the variability of the observations is given by their standard deviation (SD), SD and N_t are expressed as:

$$SD = \sqrt{\frac{\sum_{i=1}^{n}(X_{obs,i} - \overline{X}_{obs})^2}{n}} \quad (4)$$

$$N_t = \frac{SD}{RMSE} - 1 \quad (5)$$

If the value of N_t is higher than 2.2 and the value of $NSEC$ is higher than 0.90, then it can be interpreted that the model performance is very good [26], as shown in Table 2. As shown in Table 3, in the case of the Daecheong Dam, the $RMSE$ and $NSEC$ were calculated as 15.9–86.1 and 0.7–0.9, respectively, and the TIC and N_t were calculated as 0.11–0.36 and 0.69–2.99, respectively. In the case of the Gongju Weir, the $RMSE$ and $NSEC$ were calculated as 41.6–159.2 and 0.5–0.9, respectively, and the TIC and N_t were calculated as 0.16–0.25 and 0.7–1.52, respectively, suggesting "good" and "very good" model performance, respectively.

Table 2. Criteria for the goodness-of-fit evaluation [26].

Performance Rating	Model Efficiency Interpretation	N_t^a	*NSEC*
Very good	*SD* > 3.2 *RMSE*	>2.2	>0.90
Good	*SD* = 2.2 *RMSE*–3.2 *RMSE*	1.2–2.2	0.80–0.90
Acceptable	*SD* = 1.2 *RMSE*–2.2 *RMSE*	0.7–1.2	0.65–0.80
Unsatisfactory	*SD* < 1.7 *RMSE*	>0.7	<0.65

Table 3. Annual bias and *RMSE* of the control points [23].

Year	Daecheong				Gongju			
	RMSE	*NSEC*	*TIC*	N_t	*RMSE*	*NSEC*	*TIC*	N_t
2001	20.9	0.8	0.18	1.21	41.6	0.5	0.22	0.70
2002	186.1	0.7	0.36	0.69	115.7	0.6	0.25	0.86
2003	150.6	0.8	0.21	1.39	150.6	0.8	0.21	0.84
2004	124.2	0.7	0.27	0.97	129.6	0.8	0.22	0.86
2005	77.4	0.8	0.2	1.37	84.3	0.8	0.18	1.23
2006	94.7	0.9	0.19	1.76	159.2	0.8	0.23	0.69
2007	75	0.9	0.17	1.99	103.4	0.9	0.17	1.48
2008	15.9	0.9	0.11	2.99	97.3	0.9	0.16	1.52

After applying the hydrological information to the SSARR model, the simulation results were used to analyze the hydrological balance. The period 2001–2007 was used for the simulation period, because it includes the main drought year (2001) and the flood year (2003). A water balance analysis was performed in yearly increments for the seven years, based on the simulation results for the Geum River Basin (Table 4). The yearly rainfall in the Geum River Basin for the past 23 years ranged from 690 to 1758 mm, and the yearly mean rainfall was 1250 mm, which is similar to the national yearly mean rainfall. During the seven-year analysis period, 2001 had the lowest annual rainfall at 850 mm, corresponding to extreme drought. The annual rainfall in 2003 was 1459 mm, corresponding to a flood year. The results of the water balance analysis in Table 4 for the drought year of 2001 show that the loss rate was 11% higher than the mean value, and, among the runoff amounts, it had the highest runoff ratio of subsurface return water. Conversely, the results of the water balance analysis for the flood year of 2003 show that the loss rate was 4% smaller than the mean value, and, among the runoff amounts, that the amount attributable to sub-surface runoff accounted for the greatest proportion.

Table 4. Results of water balance analysis 2001–2007.

Year	Mean of Rainfall (10^6 m^3)	Unit	Losses (10^6 m^3)		Runoff (10^6 m^3)				
			Intercept	Evaporation	Surface	Sub-Surface	Base Flow	Lower Zone	Total
2001	8813	10^6 m^3	2163.0	3447.0	391.9	924.7	884.9	1464.7	3666.1
		%	25.0	39.0	4.0	10.0	10.0	17.0	42.0
2002	14,221	10^6 m^3	2844.2	4897.7	1143.3	2673.3	1395.4	1357.3	6569.8
		%	20.0	34.0	8.0	19.0	10.0	10.0	46.0
2003	15,255	10^6 m^3	2955.9	4631.3	1366.7	3242.0	1908.3	1740.8	8257.9
		%	19.0	30.0	9.0	21.0	13.0	11.0	54.0
2004	14,239	10^6 m^3	2641.4	4438.1	1352.4	3095.7	1309.6	1555.0	7312.6
		%	19.0	31.0	9.0	22.0	9.0	11.0	51.0
2005	14,014	10^6 m^3	2449.3	4723.5	1252.3	2843.2	1335.2	1585.1	7015.5
		%	17.0	34.0	9.0	20.0	10.0	11.0	50.0
2006	11,405	10^6 m^3	2559.6	3700.1	917.7	2114.0	1140.0	1424.0	5595.6
		%	22.0	32.0	8.0	19.0	10.0	12.0	49.0
2007	14,489	10^6 m^3	2961.3	4569.2	1259.1	2919.7	1461.0	1411.9	7051.8
		%	20.4	31.5	8.7	20.2	10.1	9.7	49.0
Mean	12,991	10^6 m^3	2602.2	4306.3	1070.7	2482.2	1328.9	1521.2	6402.9
		%	20.0	33.0	8.0	19.0	10.0	12.0	49.0

2.3.3. Flow Duration Coefficients

The flow duration curves illustrate the relationship between the size and ranked percentages of flow measured at fixed intervals at a single point on the stream. These are sometimes used in hydrological research for hydroelectric energy development, water supply, irrigation planning/design, and water quality management [27]. Research based on the analysis of flow duration curves has been applied to various examples by many researchers in Korea. For example, Kim and Kim [28] used total pollutant management flow measurement data to perform flow duration analysis on the Nakdong River Basin. In addition, Kim et al. [29] used flow duration curve behavior characteristics to evaluate the applicability of the SSARR model, which is a basin management model. Ryu et al. [30] performed research into optimizing the coordinated operation of dams using a hedging rule on the Han River water system. Ko et al. [31] applied flow duration change analysis to evaluate ecological and hydrological changes. Kang et al. [32] evaluated pressure factors through an analysis of flow duration change characteristics caused by the Geum River Basin dams and water usage. Ahn et al. [19,23] studied the downstream flow duration characteristics caused by the operation of reservoirs and weirs with a focus on the Geum River Basin water system in relation to the multifunction weirs built as part of the Four Major Rivers Restoration Project. Equations (6)–(8) define the flow duration coefficients used to evaluate the behavior characteristics of flow duration curves:

$$C_{fd} = \frac{Q_{10}}{Q_{355}} \tag{6}$$

$$C_F = \frac{Q_1}{Q_{185}}; C_A = \frac{Q_{95}}{Q_{185}} \tag{7}$$

$$C_L = \frac{Q_{275}}{Q_{185}}; C_D = \frac{Q_{355}}{Q_{185}} \tag{8}$$

Here, Q_1, Q_{10}, Q_{95}, Q_{185}, Q_{275} and Q_{355} are the flow regime standard flows and the subscripts are the number of maintenance days per year.

2.4. Reservoir Operation Model

The HEC-ResSim model is a simulation model developed to simulate reservoirs with a variety of requirements and restrictions. It was developed partly by the United States Army Corps of Engineers Next Generation Software Development project [14]. The HEC-ResSim model was developed to support flood adjustment, water supply planning, detailed reservoir restrictions, and real-time decision-making. The program was created to optimize the operation of reservoir systems, including all water resource uses, by completely satisfying the goals of water utilization (e.g., water supply, hydroelectric power generation, and shipping) and flood control (e.g., flood adjustment), while under the various restrictions imposed by a reservoir system composed of multiple reservoirs and control points.

Under regular dam operations, it is normal to satisfy the water level requirements of the dam by performing control and flood discharges. Control discharges are performed within a range that does not exceed the discharge capacity of the reservoir or the downstream adjustment point, so that the water level does not exceed the normal pool level. The discharge is halted when the reservoir's water level is reduced to a low-water level through the excessive supply of water. Flood discharges are performed under the condition that the regulated discharge amount will not damage the downstream area and, if the dam's water level continues to rise, that the discharge amount is necessary to reduce the water level for the safety of the dam.

On the other hand, unlike dams, multifunction weirs are operated such that they can maintain a fixed water level. Ahn and Lyu [33] examined the characteristics of downstream current behavior when a weir was operated so that the landscape water level (management water level) was maintained while the excess was discharged via a fixed weir. If the downstream requirement was not supplied, a gate was operated to supplement the supply. When discharging via a fixed weir, discharge is usually undertaken in parallel for the fishways outside the weir and for small hydropower generation installations, and any shortfall in discharge capacity is compensated via the fixed weir. In multifunction weirs, unlike dams, there is no spare margin between the hydraulic structure's constant levels and the management water levels. If a freeboard is established when building a multifunction weir model, additional water storage capacity is created, and normal simulation operation is not possible. Therefore, when building a multifunction weir model, it is necessary to make the hydraulic structure's high-water level the same as the management water level, in order to avoid virtual storage amounts and to ensure that overflow occurs via the fixed weir. In addition, when entering the multifunction weir's information, it must be simulated by deleting the fixed weir and setting up a movable weir, which is the main floodgate, as well as the power generation and fishway gates. At this point, the fixed weir section's length and width must be entered precisely, and the amount of overflow via the fixed weir is calculated within the model itself.

In the network built during this research, valid reservoir capacities for the Yongdam and Daecheong dams and the Saejong, Gongju and Baekjae weirs were linked by equivalent reservoir rules that treat them as though they had single reservoir capacity, and they were operated according to each hydraulic structure's valid reservoir capacity. Figure 8 shows the coordinated operation rules between the dams, as well as between the dams and the weirs. The overall operation rules treated the reservoirs as a single system, and they analyzed the hydrological balance with consideration of state changes. Looking at each structure's standard operating rules, the flow conveyed to the Jeonju region was first discharged, and then the downstream maintenance flow was discharged. Due to the Tandem rule, if the downstream dam or weir needed additional flow, it was discharged downstream when the operating level was above the low-water level. At the Daecheong Dam, discharge was first made toward the Daejeon region, and then the dam was operated according to the valid reservoir capacity of the downstream structures in accordance with the Tandem rule.

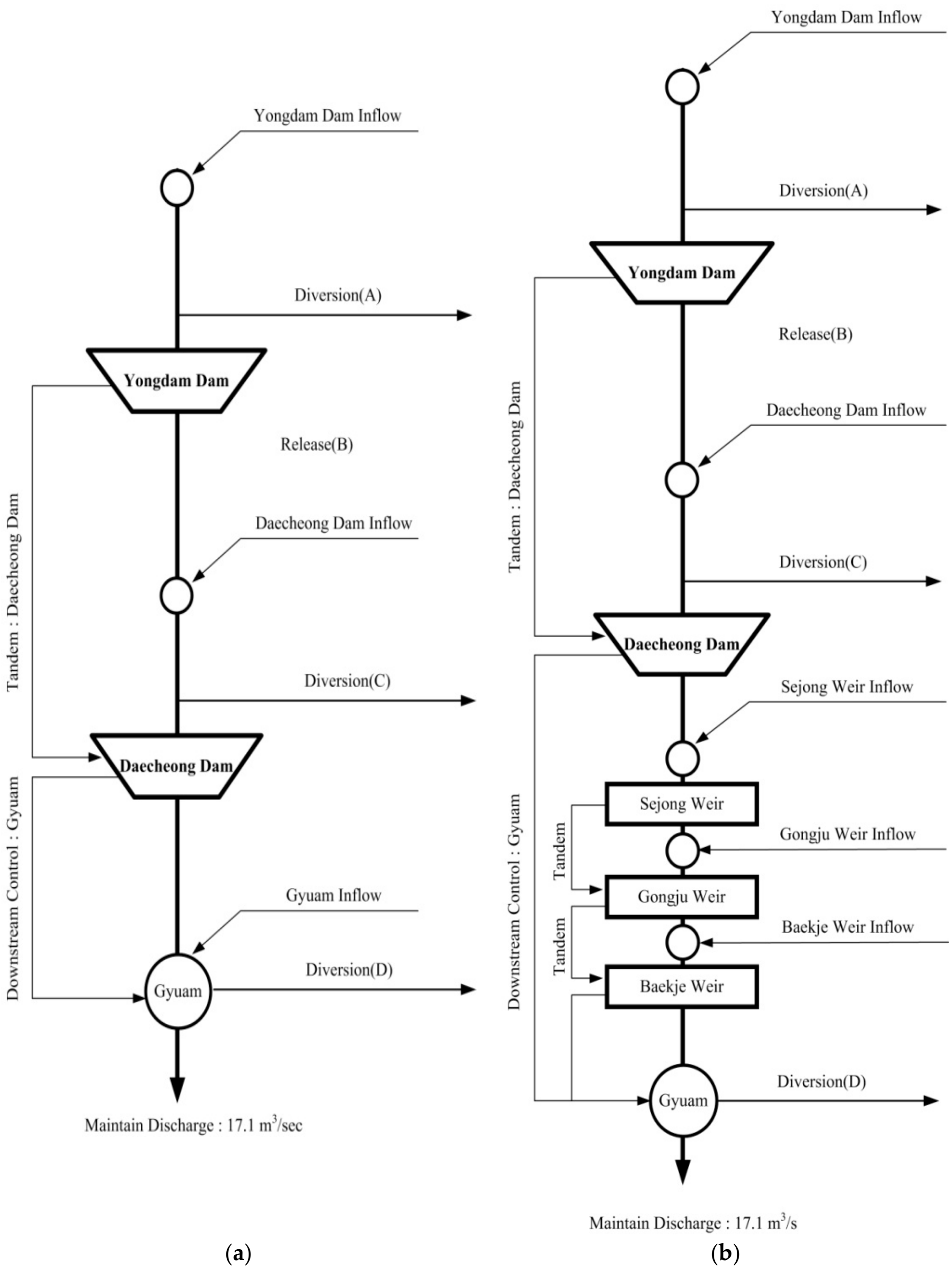

Figure 8. Operating scenarios of reservoirs and weirs: (**a**) Flowchart of operation of coupled reservoirs; (**b**) Flowchart of operation of coupled reservoirs and weirs [23].

A dam is operated such that the water level changes from the normal pool level to the low-water level. However, a multifunction weir is different to a dam, because it must be operated such that it maintains a management water level. Therefore, the very first rule was the guide curve (GC) rule. Only when the flow duration was not maintained at downstream control points were downstream discharges made, according to the Tandem rule. In Diversion (A) and Diversion (C) in Figure 8, the basic plan supplies amounts prescribed by the Dam Operation Manual [34], and it was operated such that the prescribed maintenance flow was satisfied at the Gyuam point. The dam and reservoir operation water levels were at the low-water level, and the multifunction weirs were at the stream drought water level before weir construction. The maintenance flow at the Gyuam point was made to rise by the increased flow amount that occurred when the structures were linked and operated. For streams, the stream maintenance flow 275 days before the multifunction weir was built was used as the stream drought water level. The operating water level was set to the stream drought level, assuming that the additional water impounded by the multifunction weir was equivalent to the stream drought water level deducted from the management water level.

Each structure was operated according to its GC. However, the GC, minimum desired flow, minimum release function, tandem operation, surcharge routing, and zone boundary rules (intended to match the management water levels, according to the valid low-water amounts of dams or weirs connected downstream) were applied according to the low-water amount, the downstream adjustment point's flow duration, and each point's inflow for each dam and weir built as part of the network. The Yongdam dam's constant level was EL.268.5 m, and its dam body length was 498 m. The Daecheong dam's constant level was EL.83.0 m, and its dam body length was 495 m. In the simulation, the planned flood water levels for the Yongdam and the Daecheong dams were EL.265.5 and EL.80.0 m, respectively. The normal pool levels were EL.263.5 m (January–July, November–December), 261.5 m (August–October), and EL.76.5 m. The low-water levels were EL.228.5 m and EL.60.0 m, respectively. The management water levels for the Saejong, Gongju and Baekjae weirs were EL.11.80 m, EL.8.75 m and EL.4.20 m, respectively. The low-water levels were EL.10.70 m, EL.3.28 m and EL.2.34 m, respectively. The physical data related to the power generation and operating standards are presented in Table 5.

The dam–weir operation scenario created flux data for the Gyuam gauging station, which are divided into four cases: (Case 1) no dam-weir, (Case 2) independent operation of the Yongdam and Daecheong dams, (Case 3) coordinated operation of the Yongdam and Daecheong dams, and (Case 4) coordinated operation of the Yongdam and Daecheong dams and the Sejong, Gongju and Baekjae weirs.

Table 5. Physical input data of reservoirs and weirs.

Group	Division	Specification
Yongdam	Installed Capacity	2310 kW
	Efficiency	90%
	Hydraulic Loss	1.5 m
	Max. Capacity	6.2 m^3/s
	Tailwater Elevation	EL.204 m
Daecheong	Installed Capacity	90,800 kW
	Efficiency	86%
	Hydraulic Loss	1.5 m
	Max. Capacity	264 m^3/s
	Tailwater Elevation	EL.30 m
Sejong	Installed Capacity	770 kW
	Efficiency	83.4%
	Hydraulic Loss	0.4 m
	Max. Capacity	113.4 m^3/s
	Tailwater Elevation	EL.3.2 m
Gongju	Installed Capacity	3000 kW
	Efficiency	82.72%
	Hydraulic Loss	0.35 m
	Max. Capacity	90 m^3/s
	Tailwater Elevation	EL.4.2 m
Bakje	Installed Capacity	660 kW
	Efficiency	88.0%
	Hydraulic Loss	0.4 m
	Max. Capacity	138 m^3/s
	Tailwater Elevation	EL.1.5 m

3. Results and Observations

3.1. Runoff Analysis

Climate change scenarios for South Korea with 1-km spatial resolution under RCP 4.5 and RCP 8.5 from 1 January 2006 to 31 December 2100 were applied to the basin runoff model. The runoff for each main point was calculated, with consideration given to the usage of the Geum River Basin water system. In this study, only changes in rainfall and temperature were considered, and changes in water consumption attributable to changes in land use and population were not considered.

Table 6 shows the results for the future rainfall and runoff under two RCP scenarios for comparison. In Table 6, rainfall is expressed as a sum, and runoff is a given as a mean value. Under the RCP 4.5 scenario, in comparison with the mean runoff from 2006 to 2014, the inflow rate from 2015 to 2049 increased at the Yongdam, Daecheong, Gongju and Gyuam inflow points by 13.3%, 18.6%, 23.4% and 24.6%, respectively. The inflow rate from 2050 to 2100 increased at the Yongdam, Daecheong, Gongju and Gyuam inflow points by 19.3%, 25.2%, 33.3% and 34.5%, respectively. Under the RCP 8.5 scenario, in comparison with the mean runoff from 2006 to 2014, the inflow rate from 2015 to 2049 increased at the Yongdam, Daecheong, Gongju and Gyuam inflow points by 19.2%, 16.4%, 17.5% and 16.5%, respectively. From 2050 to 2100, the inflow rate increased at the Yongdam, Daecheong, Gongju and Gyuam inflow points by 26.3%, 15.8%, 16.5% and 16.6%, respectively.

Table 6. Results of discharge calculated under RCP scenarios.

Division		2006–2014		2015–2049		2050–2100	
		Rainfall (mm)	Discharge (m^3/s)	Rainfall (mm)	Discharge (m^3/s)	Rainfall (mm)	Discharge (m^3/s)
Yongdam Inflow	RCP 4.5	3.9	26.6	4.3	30.7	4.6	33.0
	RCP 8.5	4.0	21.8	4.7	27.0	4.9	29.6
Daecheong Inflow	RCP 4.5	3.5	26.3	4.3	32.4	4.6	35.2
	RCP 8.5	3.3	24.5	4.1	29.3	4.2	29.2
Gongju	RCP 4.5	3.8	54.1	4.4	70.6	4.7	81.1
	RCP 8.5	3.6	49.4	4.2	59.9	4.5	59.2
Gyuam	RCP 4.5	3.6	42.1	4.4	95.7	4.8	110.0
	RCP 8.5	3.8	69.7	4.4	83.5	4.7	83.6

Under the RCP 4.5 scenario, a continuous trend of runoff increase was predicted. At the Yongdam and Daecheong inflow points, which correspond to the upstream region, a greater increase was predicted under the RCP 8.5 scenario than under the RCP 4.5 scenario. Conversely, for the Gongju and Gyuam inflow points, which correspond to the downstream region, a greater increase was predicted under the RCP 4.5 scenario than under the RCP 8.5 scenario.

Tables 7–10 show analyses of the monthly dam inflows for each climate change scenario. The figures in parentheses in the tables represent the ratios of increase compared with 2006–2014. It should be noted that the inflow increments for October–April are larger than for July–September, which is Korea's flood season. The summer runoff ratio is especially reduced. This reflects changes in the overall water circulation system, and it highlights the alteration of the seasonal characteristics as well as the poor distribution of available water resources. Therefore, continuous monitoring and analysis of the changes in characteristics will be needed for more efficient water resource management. If these predicted trends were to become reality in the future, it would be necessary to reexamine our reservoir operation rules and to convert to a system that could be effectively distributed so that efficient water management could be performed.

Table 7. Analysis of monthly mean inflow at 404,705 point (unit: m^3/s).

Scenario		Jan.	Feb.	Mar.	Apr.	May	Jun.	Jul.	Aug.	Sep.	Oct.	Nov.	Dec.
RCP 4.5	2006–2014	5.8	14.2	12.1	17.8	17.8	19.6	93.1	73.7	43.5	6.2	4.8	8.5
	2015–2055	7.7 (0.32)	11.4 (−0.20)	17.0 (0.41)	18.0 (0.01)	24.9 (0.40)	31.0 (0.58)	139.9 (0.50)	62.2 (−0.15)	27.0 (−0.38)	6.4 (0.03)	8.2 (0.69)	11.2 (0.31)
	2056–2100	9.9 (0.69)	12.4 (−0.13)	18.5 (0.53)	28.5 (0.60)	24.1 (0.35)	29.5 (0.51)	141.8 (0.52)	70.0 (−0.05)	32.5 (−0.25)	7.7 (0.23)	8.7 (0.81)	10.5 (0.23)
RCP 8.5	2006–2014	4.4	6.6	11.6	16.8	17.8	32.4	80.5	40.6	35.8	5.5	3.6	4.6
	2015–2055	8.8 (1.00)	8.3 (0.27)	15.7 (0.35)	25.7 (0.53)	27.0 (0.52)	34.9 (0.08)	96.1 (0.19)	54.0 (0.33)	23.9 (−0.33)	7.8 (0.43)	9.7 (1.69)	9.6 (1.09)
	2056–2100	7.8 (0.76)	14.9 (1.27)	18.2 (0.56)	30.2 (0.80)	26.9 (0.51)	49.4 (0.52)	104.2 (0.29)	46.8 (0.15)	27.8 (−0.22)	8.6 (0.56)	9.2 (1.53)	8.6 (0.87)

Table 8. Analysis of monthly mean inflow at 404,714 point (unit: m^3/s).

Scenario		Jan.	Feb.	Mar.	Apr.	May	Jun.	Jul.	Aug.	Sep.	Oct.	Nov.	Dec.
RCP 4.5	2006–2014	7.1	12.7	13.2	18.9	16.9	18.5	87.3	66.3	46.0	9.9	7.8	9.8
	2015–2055	8.7 (0.24)	10.5 (−0.18)	16.9 (0.28)	18.6 (−0.01)	23.6 (0.39)	34.5 (0.86)	151.4 (0.74)	60.9 (−0.08)	28.0 (−0.39)	10.2 (0.03)	10.2 (0.30)	11.8 (0.20)
	2056–2100	10.9 (0.54)	12.7 (0.00)	19.1 (0.44)	29.3 (0.55)	28.8 (0.70)	42.2 (1.28)	141.8 (0.62)	70.1 (0.06)	31.9 (−0.31)	11.8 (0.19)	10.6 (0.36)	10.7 (0.09)
RCP 8.5	2006–2014	5.6	8.5	12.1	14.9	16.9	26.2	95.0	53.0	38.9	8.7	6.3	6.6
	2015–2055	12.0 (1.15)	12.0 (0.41)	18.4 (0.51)	26.1 (0.76)	24.4 (0.44)	41.9 (0.60)	92.4 (−0.03)	58.2 (0.10)	27.7 (−0.29)	12.4 (0.43)	11.9 (0.89)	12.8 (0.95)
	2056–2100	10.7 (1.15)	18.6 (0.41)	20.8 (0.51)	27.8 (0.76)	24.3 (0.44)	34.8 (0.60)	98.2 (−0.03)	49.9 (0.10)	31.1 (−0.29)	10.8 (0.43)	10.5 (0.89)	10.5 (0.95)

Table 9. Analysis of monthly mean inflow at 404,721 point (unit: m^3/s).

Scenario		Jan.	Feb.	Mar.	Apr.	May	Jun.	Jul.	Aug.	Sep.	Oct.	Nov.	Dec.
RCP 4.5	2006–2014	21.8	27.6	25.8	35.8	33.3	30.7	161.3	117.2	100.8	33.4	29.5	28.4
	2015–2055	26.5 (0.21)	26.4 (−0.04)	32.3 (0.25)	35.2 (−0.02)	43.7 (0.31)	70.5 (1.29)	304.4 (0.89)	127.3 (0.09)	69.6 (−0.31)	37.1 (0.11)	34.7 (0.18)	33.3 (0.17)
	2056–2100	30.9 (0.42)	31.5 (0.14)	38.7 (0.50)	56.8 (0.59)	57.4 (0.73)	80.8 (1.63)	322.8 (1.00)	154.9 (0.32)	77.1 (−0.24)	41.7 (0.25)	37.7 (0.28)	33.2 (0.17)
RCP 8.5	2006–2014	17.6	19.5	22.1	26.1	27.5	46.2	179.6	97.0	77.2	28.6	25.2	23.3
	2015–2055	31.1 (0.76)	28.7 (0.47)	36.0 (0.63)	48.9 (0.87)	46.8 (0.70)	78.8 (0.70)	174.7 (−0.03)	106.4 (0.10)	59.7 (−0.23)	36.8 (0.29)	34.9 (0.39)	33.1 (0.42)
	2056–2100	28.5 (0.76)	39.9 (0.47)	39.6 (0.63)	51.0 (0.87)	47.8 (0.70)	63.2 (0.70)	191.8 (−0.03)	85.3 (0.10)	62.4 (−0.23)	34.1 (0.29)	32.7 (0.39)	29.6 (0.42)

Table 10. Analysis of monthly mean inflow at 404,723 point (unit: m^3/s).

Scenario		Jan.	Feb.	Mar.	Apr.	May	Jun.	Jul.	Aug.	Sep.	Oct.	Nov.	Dec.
RCP 4.5	2006–2014	29.2	37.1	35.5	49.4	47.2	41.1	213.8	150.8	134.3	45.0	39.9	38.4
	2015–2055	35.7 (0.22)	35.6 (−0.04)	43.7 (0.23)	48.2 (−0.02)	60.4 (0.28)	96.3 (1.34)	421.3 (0.97)	164.2 (0.09)	92.8 (−0.31)	50.1 (0.11)	46.9 (0.17)	44.7 (0.16)
	2056–2100	41.4 (0.42)	42.2 (0.14)	52.5 (0.48)	76.8 (0.55)	79.5 (0.68)	113.8 (1.77)	439.2 (1.05)	205.5 (0.36)	104.4 (−0.22)	56.6 (0.26)	51.3 (0.29)	45.0 (0.17)
RCP 8.5	2006–2014	24.9	26.9	30.8	36.7	38.5	65.8	252.6	134.7	112.1	40.7	35.7	32.8
	2015–2055	42.2 (0.70)	38.7 (0.44)	48.3 (0.57)	66.1 (0.80)	64.0 (0.66)	106.4 (0.62)	249.0 (−0.01)	153.0 (0.14)	84.7 (−0.24)	51.4 (0.26)	48.4 (0.36)	45.2 (0.38)
	2056–2100	39.0 (0.57)	53.4 (0.99)	53.3 (0.73)	71.5 (0.95)	65.8 (0.71)	89.7 (0.36)	276.0 (0.09)	124.2 (−0.08)	88.8 (−0.21)	48.2 (0.18)	45.6 (0.28)	40.9 (0.25)

The parameter C_{fd} in Equation (6) is a flow regime coefficient proposed by Lee et al. [35], which is a criterion of the change in the flow duration. It can be said to have the same meaning as a flow duration coefficient. Thus, as the flow duration coefficient C_{fd} increases, the change in flow becomes larger. Conversely, as it decreases, the change in flow becomes smaller and the flow becomes more stable. The parameters C_F and C_A in Equation (7) are flood water and rain water coefficients proposed by Park [36] that have values >1. As these values become smaller, the rain water amount Q_{95} or flood water amount Q_1 become closer to the normal water amount Q_{185}, i.e., they show the extent to which the stream flow is above the normal water amount. As the flood water coefficient C_F and the rain water coefficient C_A become larger, the flood water amount Q_1 and the rain water amount Q_{95} become closer to the normal water amount Q_{185}. Therefore, the flow of a big flood will be similar in size to the rain water amount Q_{95}. The parameters C_L and C_D in Equation (8), proposed by Park (2003), represent a low-water coefficient and a drought water coefficient, respectively, and their values are <1. The low-water coefficient and the drought water coefficient represent a quantified ratio of the low-water amount Q_{275} and the drought water amount Q_{355} to the normal amount Q_{185}. They are used as information for making decisions about water resource development/management and about the stream's ecology and environment. As the low-water coefficient C_L and the drought water coefficient C_D become larger, the low-water amount Q_{275} and the drought water amount Q_{355} become similar in size to the normal water amount Q_{185}.

Table 11 shows the flow regime coefficients and Table 12 shows the flow regime standard flows. Table 11 shows that a smaller C_{fd} was calculated under RCP 8.5 than under RCP 4.5, and that it was at its smallest (19.7) at the Gyuam point. The flow regime coefficients were higher in the upstream area than in the downstream area. This means that it might be difficult to continuously develop and manage water resources as the changes in the amount of water in the stream gradually increase. Overall, there was little difference between the low-water coefficient and the drought water coefficient under the RCP 4.5 scenario compared with the RCP 8.5 scenario; however, the flood water coefficient C_F and the rain water coefficient C_A values were higher. When this was compared with the flow duration analyzed via the observed data from 2006 to 2014, the entire flow duration was increased under the RCP scenarios. Under RCP 8.5, the flow was reduced in the flood season compared with RCP 4.5. Furthermore, Table 12 shows that extreme flow (Q_1) occurrences were reduced. In the case of Korea, where rainfall occurs mostly in the summer, the flow is impounded in the flood season and used in the growing season, which might cause problems for Korea's irrigation requirements. Therefore, it will be necessary to adequately predict the runoff amount that might occur with climate change and to gather the basic information necessary for establishing a long-term plan for future dam operations.

Table 11. Coefficient of flow regime characteristics calculated at each point.

Point	Scenario	C_{fd}	C_F	C_A	C_L	C_D
Yongdam Inflow	RCP 4.5 RCP 8.5	108.2 129.1	59.7 69.9	2.3 2.3	0.5 0.4	0.2 0.1
Daecheong Inflow	RCP 4.5 RCP 8.5	52.5 41.2	68.9 51.3	2.0 1.9	0.6 0.6	0.4 0.3
Gongju	RCP 4.5 RCP 8.5	27.7 19.1	47.6 34.6	1.5 1.5	0.7 0.8	0.5 0.6
Gyuam	RCP 4.5 RCP 8.5	27.7 19.7	47.7 34.6	1.4 1.5	0.7 0.8	0.5 0.5

Table 12. Analysis of the duration curve at each point (m^3/s).

Point	Scenario	Q_1	Q_{10}	Q_{95}	Q_{185}	Q_{275}	Q_{355}
ngdam Inflow	RCP 4.5 RCP 8.5	680.7 692.9	202.7 181.4	25.7 22.4	11.4 9.9	5.3 4.1	1.9 1.4
Daecheong Inflow	RCP 4.5 RCP 8.5	797.5 623.6	226.3 172.2	23.4 22.8	11.6 12.1	7.0 7.2	4.3 4.2
Gongju	RCP 4.5 RCP 8.5	1,534.1 1,034.2	484.2 320.5	46.8 43.4	32.2 29.9	23.6 22.8	17.5 16.8
Gyuam	RCP 4.5 RCP 8.5	2,102.1 1,440.5	647.8 450.5	63.9 61.2	44.1 41.7	32.1 31.5	23.4 22.8

3.2. Analysis of Discharge Amount and of Power Generation Amount

The runoff results calculated using the SSARR model, based on the observed rainfall from 1985 to 2008, and the runoff results calculated under the RCP 4.5 and RCP 8.5 scenarios were applied to the HEC-ResSim model to calculate the power generation under each scenario.

As shown in Figures 9 and 10, the results of the flow duration analysis at Gyuam show that, for a drought water amount of Q95% (the 5 percentile flow; the flow in cubic meters per second which was equalled or exceeded for 95% of the flow record.), Cases 1–4 under the RCP 4.5 scenario were 27, 28, 34 and 35 m^3/s, respectively, while, under the RCP 8.5 scenario, Cases 1–4 were 25.4, 33.9, 34.1 and 35.6 m^3/s, respectively. Compared with RCP 4.5, the amount of flow under RCP 8.5 that could be maintained in the stream during the drought period increased, but the effect of coordinated operation was greater under RCP 4.5 than under RCP 8.5. This is believed to reflect greater flow in the Yongdam dam under RCP 4.5 than under RCP 8.5, such that the effect of the coordinated operation is increased, as shown in Figures 9 and 10. In terms of generation, Table 13 shows that, under the climate change scenarios, the generation amount was reduced compared with the past. More power generation could be achieved under RCP 4.5 than under RCP 8.5, and, when the reservoirs and weirs were linked, greater generation could be achieved. Therefore, even under the effects of climate change, the risk to power generation could be reduced through the coordinated operation of reservoirs and weirs.

Since future hydrological data are data that are predicted based on information that includes several types of uncertainty, the predicted results are not representative of a precise period. Essentially, taking past data and predicting the future inherently includes some degree of limitation and uncertainty. As we are analyzing a complex world with only statistical methods and a limited number of factors, it is difficult to make accurate predictions about climate change. However, it is clear that climate change is occurring. Therefore, we believe it is necessary to evaluate runoff and the effects that might occur because of overall changes in the hydrological environment that may be attributable to climate change. We believe that, in the future, this research will be helpful for establishing a water resource distribution/management strategy in response to climate change.

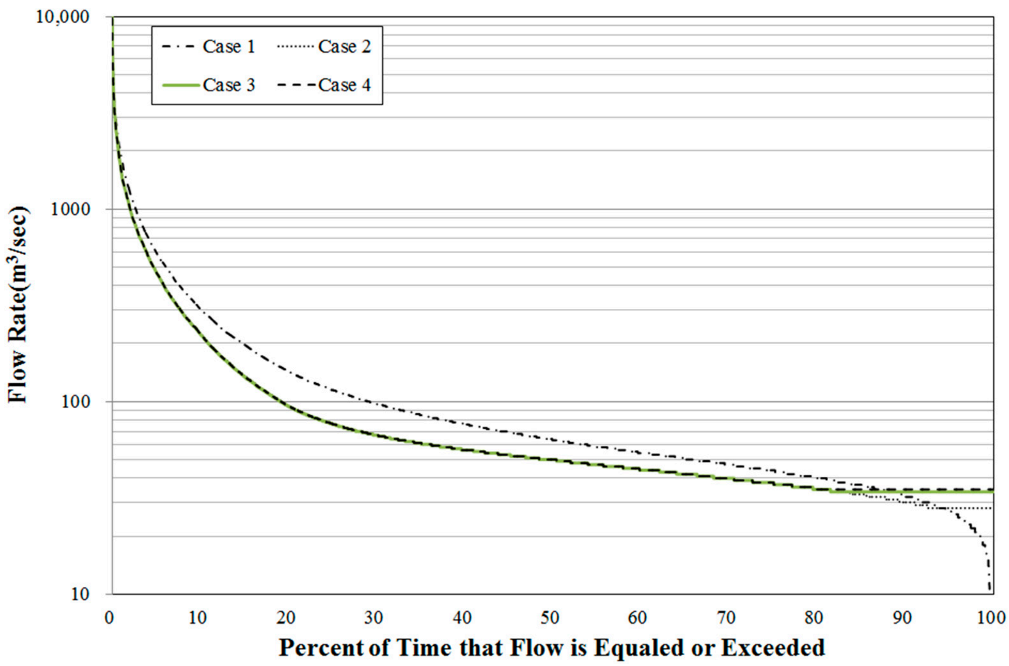

Figure 9. Flow duration curve at the Gyuam point estimated under RCP 4.5.

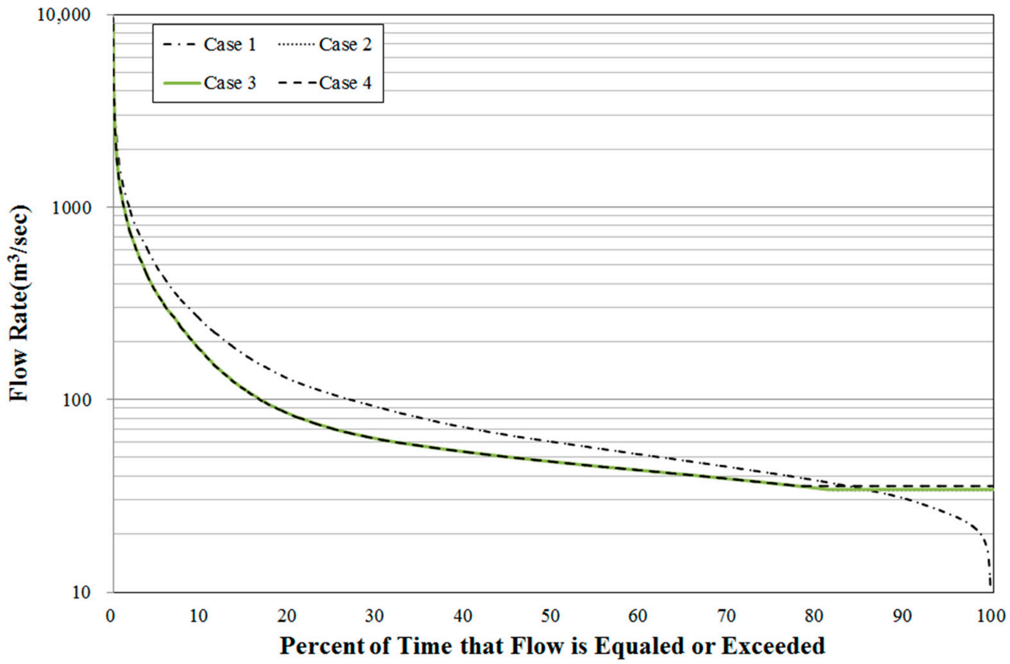

Figure 10. Flow duration curve at the Gyuam point estimated under RCP 8.5.

Table 13. Comparison of generation under each scenarios (unit: GWh).

Group		Case 2	Case 3	Case 4
1985–2008	Generation (GWh)	60.33	60.77	60.81
RCP 4.5	Generation (GWh)	41.06	41.87	42.03
RCP 8.5	Generation (GWh)	38.98	39.12	40.99

4. Conclusions

In this research, we used the RCP climate change scenarios provided by the Korea Meteorological Association to analyze the future runoff characteristics and power generation of the Geum River Basin from 2006 to 2100. Based on the results of our analyses, we derived the following conclusions:

(1) The results of analyzing the monthly dam inflow for each climate change scenario showed that the inflow increments for October–April were larger than the inflow increments for the flood season (July–September). We believe this means there will be changes to the entire water circulation system due to climate change, which could explain both the appearance of seasonal characteristics that differ from before and the poor distribution of available water resources.

(2) Under the RCP 4.5 and RCP 8.5 scenarios, there was little difference in the low-water and drought water coefficients. However, under the RCP 4.5 scenario, the flood water coefficient C_F was higher than the rain water coefficient C_A, which means that, under the RCP 8.5 scenario, the flow during the flood season was reduced. In the case of Korea, considered a country with insufficient water resources, the river regime coefficient was large. This means rain water is mainly stored in reservoirs and weirs during the summer, and insufficient water resources are supplemented as necessary by discharging downstream; however, as flood season runoff might be reduced, a new water resource management plan will be needed.

(3) In terms of power generation, it was found that the power generation was reduced compared with the past under the climate change scenarios. Under RCP 4.5, more power generation was achieved than under RCP 8.5, and, when the operations of the reservoirs and weirs were coordinated, even more power generation was achieved. Therefore, even if climate change occurs, the risk to power generation could be reduced by the coordinated operation of reservoirs and weirs.

(4) In order to examine quantitatively the changing stream environment in the future, we must implement flow and water quality monitoring projects to obtain observational data related to our numerical simulations. In addition, we believe there is need for analysis that reflects basin runoff characteristics, including existing dams and newly constructed multifunction weirs, for which assessments of the future river environment must be performed.

Acknowledgments: This research was funded by the National Institute of Environmental Research of Korea.

Author Contributions: The manuscript was written by Jung Min Ahn and he was mainly responsible for the initial research proposal, field work, consultations, survey and numerical design and policy analysis, but all authors contributed to its preparation and review. Deuk Seok Yang and Kang Young Jung were mainly responsible for designing and implementing the web-based survey and hydrologic modeling portions of the manuscript. Dong Seok Shin revised the language and edited the first draft and did the final overall proof reading of the manuscript.

Conflicts of Interest: The authors declare no conflict of interest.

References

1. Intergovernmental Panel on Climate Change (IPCC). *Climate Change 2007—The Physical Science Basis: Contributions of Working Group I to the Fourth Assessment Report of the Intergovernmental Panel on Climate Change*; Cambridge University Press: Cambridge, UK; New York, NY, USA, 2007.
2. Park, C.; Moon, J.; Cha, E.; Yun, W.; Choi, Y. Recent changes in summer precipitation characteristics over South Korea. *J. Korean Geogr. Soc.* **2008**, *43*, 324–336. (In Korean)
3. Korea Environment Institute. *River Management and Ecological Restoration in Response to Climate Change*; Korea Environment Institute: Seoul, Korea, 2012. (In Korean)
4. National Institute of Environmental Research. *Plans Prepared for Climate Change; a White Paper and Basic Research*; National Institute of Environmental Research: Incheon, Korea, 2008. (In Korean)
5. National Institute of Environmental Research. *Integrated Impact Assessment of Climate Change on Watershed Environment*; National Institute of Environmental Research: Incheon, Korea, 2010. (In Korean)
6. Korea Rural Economic Institute. *Response to Climate Change in Agriculture*; Korea Rural Economic Institute: Naju, Korea, 2011. (In Korean)
7. Chung, E.; Lee, J.; Ko, I.W. California water plan; Integrated water management. *Mag. Korea Water Res. Assoc.* **2011**, *43*, 76–82. (In Korean)
8. Chung, E.; Lee, G.; Lee, K. Introduction of APFM and Integrated Flood Management concept and apply. *Mag. Korea Water Res. Assoc.* **2009**, *41*, 70–78. (In Korean)
9. Lee, J.; Kim, Y.; Lee, K. A study on combining climate change scenarios. In *2009 Proceedings of the Korean Society of Civil Engineers*; Korean Society of Civil Engineers: Seoul, Korea, 2009; pp. 621–626. (In Korean)
10. Inha University. *Ministry of Land, Transport and Maritime Affairs, Development Study Report for Assessment Techniques on over the Flood*; Inha University: Incheon, Korea, 2007. (In Korean)
11. Ministry of Science and Technology. *The 21st Century Frontier R&D Program; Sustainable Water Resources Research Program; Technology for Climate Change Impact Assessment on Water Resources*; Ministry of Science and Technology: Gwacheon, Korea, 2007. (In Korean)
12. K-water Institute. *Derived from the Research for Countermeasures to Climate Change for Future Water Management Plan*; K-water Institute: Daejeon, Korea, 2010. (In Korean)
13. Minville, M.; Brissette, F.; Leconte, R. Impacts and uncertainty of climate change on water resource management of the Peribonka River System (CANADA). *J. Water Res. Plan. Manag. ASCE* **2010**, *136*, 376–385. [CrossRef]
14. Klipsch, J.D.; Hurst, M.B. *HEC-ResSim, Reservoir System Simulation User's Manual*; Version 3.0.; U.S. Army Corps of Engineers, Institute for Water Resources, Hydrologic Engineering Center: Davis, CA, USA, 2007.
15. Fang, H.; Cheong, Y.; Yan, S. Optimization on water resource system operation policy during drought. *J. Water Res. Protection* **2011**, *3*, 140–156. [CrossRef]
16. Divakar, L.; Babel, M.S.; Perret, S.R.; Gupta, A.D. Optimal allocation of bulk water supplies to competing use sectors based on economic criterion—An application to the Chao Phraya River Basin, Thailand. *J. Hydrol.* **2011**, *401*, 22–35. [CrossRef]

17. Lin, N.M.; Rutten, M. Optimal operation of a network of multi-purpose reservoir: A review. *Procedia Eng.* **2016**, *154*, 1376–1384. [CrossRef]
18. Li, Y.; Cui, Q.; Li, C.; Wang, X.; Cai, Y.; Cui, G.; Yang, Z. An improved multi-objective optimization model for supporting reservoir operation of China's South-to-North water diversion project. *Sci. Total Environ.* **2017**, *575*, 970–981. [CrossRef] [PubMed]
19. Ahn, J.M.; Lee, S.J.; Kang, T. Evaluation of dams and weirs operating for water resource management of the Geum River. *J. Sci. Total Environ.* **2014**, *478*, 103–115. [CrossRef] [PubMed]
20. Climate Change Information Center. 2013. Available online: www.climate.go.kr (accessed on 14 April 2013).
21. Korea Meteorological Administration. *Climate Change Handbook*; Korea Meteorological Administration: Seoul, Korea, 2010. (In Korean)
22. Intergovernmental Panel on Climate Change (IPCC). *Climate Change 2013—The Physical Science Basis. Contribution of Working Group I to the Fifth Assessment Report of the Intergovernmental Panel on Climate Change*; Cambridge University Press: Cambridge, UK; New York, NY, USA, 2013.
23. Ahn, J.M.; Jung, K.Y.; Shin, D.S. Effects of coordinated operation of weirs and reservoirs on the water quality of the Geum River. *Water* **2017**, *423*, 1–27.
24. Nash, J.E.; Sutcliffe, J.V. River flow forecasting through conceptual models part I. A discussion of principles. *J. Hydrol.* **1970**, *10*, 282–290. [CrossRef]
25. Christiansen, D.E. *Simulation of Daily Streamflows at Gaged and Ungagged Locations within the Cedar River Basin, Iowa, Using a Precipitation-Runoff Modeling System Model*; U.S. Scientific Investigations Report; U.S. Geological Survey: Reston, VA, USA, 2012; pp. 2012–5213.
26. Ritter, A.; Munoz-Carpena, R. Performance evaluation of hydrological models: Statistical significance for reducing subjectivity in goodness-of-fit assessments. *J. Hydrol.* **2013**, *480*, 33–45. [CrossRef]
27. Maidment, D.R. *Handbook of Hydrology*; McGraw-Hill: New York, NY, USA, 1992; pp. 53–54.
28. Kim, J.C.; Kim, S. Flow duration curve analysis for Nakdong River Basin using TMDL flow data. *J. Korean Soc. Water Qual.* **2007**, *23*, 332–338. (In Korean)
29. Kim, J.C.; Lee, S.J.; Shin, H.H.; Hwang, M.H. The evaluation of watershed management model using behavioral characteristics of flow-duration curve. *J. Korean Soc. Water Qual.* **2009**, *25*, 573–579. (In Korean)
30. Ryu, G.; Chung, G.; Lee, J.H.; Kim, J.H. Optimization of multi-reservoir operation with a hedging rule: Case study of the Han River Basin. *J. Korea Water Res. Assoc.* **2009**, *42*, 643–657. (In Korean) [CrossRef]
31. Ko, I.; Kim, J.; Park, S. Evaluation of eco-hydrological changes in the Geum River considering dam operation: I. flow regime change analysis. *J. Korea Water Res. Assoc.* **2009**, *42*, 1–8. (In Korean) [CrossRef]
32. Kang, S.K.; Lee, D.; Moon, J.W.; Choi, S.J. Effects of dams and water use on flow regime alteration of the Geum River Basin. *J. Korea Water Res. Assoc.* **2010**, *43*, 325–336. (In Korean) [CrossRef]
33. Ahn, J.M.; Lyu, S. Analysis of the coordinated operation of reservoirs and weirs during the management of Nakdong River water resources. *J. Water Res. Plan. Manag.* **2017**, 143. [CrossRef]
34. Korea Water Resources Corporation (K-water). *Practical Manual of Dam, Korea Water Resources Corporation*; Korea Water Resources Corporation (K-water): Daejeon, Korea, 2012. (In Korean)
35. Lee, J.W.; Kim, H.S.; Woo, H.S. An analysis of the effect of damming on flow duration characteristics of five major rivers in Korea. *J. Korean Soc. Civil Eng.* **1993**, *13*, 79–91. (In Korean)
36. Park, S.D. Dimensionless flow duration curve in natural river. *J. Korea Water Res. Assoc.* **2003**, *36*, 33–44. (In Korean) [CrossRef]